Author(s): Vattulainen, I. & Ying, S. C. & Ala-Nissilä, Tapio & Merikoski, J.

Title: Memory effects and coverage dependence of surface diffusion in a model adsorption system

Year: 1999

Version: Final published version

Please cite the original version:

Vattulainen, I. & Ying, S. C. & Ala-Nissilä, Tapio & Merikoski, J. 1999. Memory effects and coverage dependence of surface diffusion in a model adsorption system. Physical Review B. Volume 59, Issue 11. P. 7697-7707. ISSN 1098-0121 (printed). DOI: 10.1103/physrevb.59.7697.

Memory effects and coverage dependence of surface diffusion in a model adsorption system

I. Vattulainen*
Helsinki Institute of Physics, P.O. Box 9 (Siltavuorenpenger 20 C), FIN–00014 University of Helsinki, Finland

S. C. Ying
Helsinki Institute of Physics, P.O. Box 9 (Siltavuorenpenger 20 C), FIN–00014 University of Helsinki, Finland and Department of Physics, Box 1843, Brown University, Providence, Rhode Island 02912

T. Ala-Nissila
Helsinki Institute of Physics, P.O. Box 9 (Siltavuorenpenger 20 C), FIN–00014 University of Helsinki, Finland; Department of Physics, Box 1843, Brown University, Providence, Rhode Island 02912; and Laboratory of Physics, Helsinki University of Technology, P.O. Box 1100, FIN–02015 HUT, Finland

J. Merikoski
Department of Physics, University of Jyväskylä, P.O. Box 35, FIN–40351 Jyväskylä, Finland
(Received 1 September 1998)

We study the coverage dependence of surface diffusion coefficients for a strongly interacting adsorption system O/W(110) via Monte Carlo simulations of a lattice-gas model. In particular, we consider the nature and emergence of memory effects as contained in the corresponding correlation factors in tracer and collective diffusion. We show that memory effects can be very pronounced deep inside the ordered phases and in regions close to first and second order phase transition boundaries. Particular attention is paid to the details of the time dependence of memory effects. The memory effect in tracer diffusion is found to decay following a power law after an initial transient period. This behavior persists until the hydrodynamic regime is reached, after which the memory effect decays exponentially. The time required to reach the hydrodynamical regime and the related exponential decay is strongly influenced by both the critical effects related to long-wavelength fluctuations and the local order in the overlayer. We also analyze the influence of the memory effects on the effective diffusion barriers extracted from the Arrhenius analysis. For tracer diffusion, we find that the contribution from memory effects can be as large as 50% to the total barrier. For collective diffusion, the role of memory effects is in general less pronounced. [S0163-1829(99)03011-8]

I. INTRODUCTION

Surface diffusion plays a fundamental role in various physically and technologically important processes. Surface growth under molecular beam epitaxy conditions[1] and chemical reactions[2] are just two examples of situations where single-particle motion as characterized by tracer diffusion[3,4] is one of the most important underlying microscopic mechanisms. On the other hand, relaxation of surfaces after growth or sputtering[5] via mass transport can be characterized by collective diffusion. [3,4] There is therefore an obvious desire to understand the basic principles that govern diffusion. In the case of single-particle diffusion at very low coverages, significant progress has been made based on microscopic approaches,[4,6–11] while for finite coverages and strong interactions much less has been achieved.

Perhaps the most commonly used theoretical approach in studying surface diffusion is the lattice-gas model.[12,13] Within the lattice-gas model, diffusion of adsorbed particles takes place via thermally activated jumps between discrete adsorption sites on a lattice. Despite its simplified nature, the lattice-gas model provides a reasonably good approximation for many adsorption systems.[5,13] However, this is true only if the appropriate dynamical algorithm for the transition between different system configurations is adopted. [14] Within this approach, the tracer diffusion coefficient D_T can be expressed formally as a product of the average single-particle transition rate Γ and the correlation factor f_T, which accounts for all the *memory effects* arising from correlations between consecutive displacements of a tagged particle.[13,15,16] The collective diffusion coefficient D_C can be similarly expressed as a product of Γ and the correlation factor f_C accounting for the memory effects in the center-of-mass motion of the diffusing particles, and an additional contribution due to thermodynamic particle number fluctuations.[13,15,16]

Previous theoretical works for interacting adsorption systems have mainly focused on how the diffusion coefficients D_T and D_C depend on thermodynamic conditions such as the presence of ordered phases and phase transition boundaries.[4,17–26] Of special interest has been the behavior of the prefactor and the diffusion barrier extracted from an Arrhenius analysis of the temperature dependence of the diffusion coefficients. [3,5,17,18,21,22,27–31] However, the actual *microscopic origins* of the prefactor and the effective activation barrier are poorly understood. This is particularly true as regards the memory effects, all of which in the lattice-gas description are contained in the correlation factors f_T and f_C. In the case of single-particle diffusion, memory effects arising from the substrate vibrations have been shown to

increase the Arrhenius barrier from its static (bare) value.[32] In the case of many-particle diffusion in an interacting system, where there is often no microscopic justification for Arrhenius behavior,[33] this issue is obviously much more complicated.

The purpose of this work is to systematically consider the origin and implications of memory effects in different parts of the phase diagram of a strongly interacting model system. A brief report of some of the results can be found in Ref. 34. We employ Monte Carlo simulations to study the coverage dependence of tracer and collective diffusion in a lattice-gas model of O/W(110).[33,35] Using a formal decomposition of the diffusion coefficients, we extract the contribution of memory effects from the data as contained in the correlation factors. We find very pronounced memory effects in ordered phases and close to first and second order phase transition boundaries. The time to reach the hydrodynamical regime, where Fick's laws are valid and where the diffusion coefficients are therefore defined, is also found to depend strongly on the presence of ordered phases and critical fluctuations. The decay of memory effects is then studied in more detail at short and intermediate time scales by examining direct correlations between successive jumps of a tagged particle. After an initial transient period but prior to the onset of the hydrodynamic regime, we find strong evidence that the single-particle memory effect decays according to a power law. At times beyond the onset of the hydrodynamic regime, our results are consistent with an exponential decay.

To make contact with previous studies and experiments, we also analyze the temperature dependence of memory effects using the conventional Arrhenius analysis. We find that the effective diffusion barrier E_A of tracer diffusion is strongly influenced by memory effects at finite coverages and low temperatures, where about 10–50 % of E_A arises from temperature variations in the memory effects. It is only the remaining part that is directly connected to thermally activated single-particle jumps as described by the average transition rate Γ. In the case of collective diffusion, the memory contribution to the Arrhenius barrier is also important but less pronounced. Finally, we shall discuss our results in light of the recent theoretical work[36] and existing experimental data for the system in question.[37]

II. LATTICE-GAS MODEL OF O/W(110)

In the lattice-gas model employed in this work, the interaction parameters are chosen[33,35] such that the resulting phase diagram shown in Fig. 1 is in close agreement with the experimental observations[38–40] for the O/W(110) system. We note that the theoretical phase diagram does not describe all the features of the real adsorption system with quantitative accuracy. However, the purpose of the present work is not to study the quantitative features of the O/W(110) system but rather to study effects on the adatom dynamics arising from strong interactions and collective effects in general.

In a study of dynamical properties such as diffusion coefficient, the specification of the interaction parameters in the lattice-gas Hamiltonian is not alone sufficient. The results also depend on the choice of transition probabilities $w_{i,f}$ from an initial state i with energy E_i to a final state f with energy E_f.[14] As explained in Ref. 33, in addition to the usual

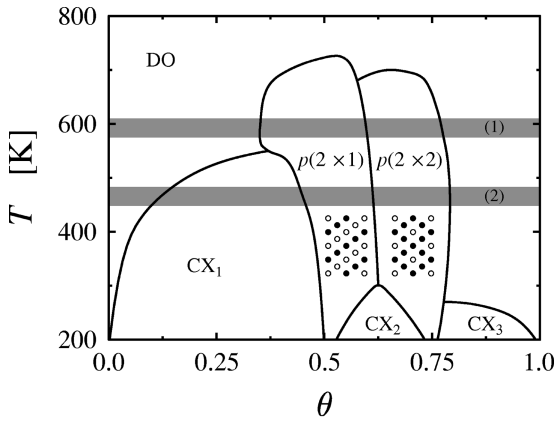

FIG. 1. A schematic phase diagram of the O/W(110) system in the T-θ plane. DO denotes the disordered region, $p(2\times1)$ and $p(2\times2)$ denote the ordered phases, and CX_i with $i=1,2,3$ are coexistence phases. Configuration snapshots of ideal ordered phases are also shown, the occupied and vacant adsorption sites being denoted by filled and open circles, respectively. The temperature regimes (1) and (2) [see Sec. II] studied in this work are shaded with gray. We stress that although the present phase diagram is more accurate than the one given in a previous work (Ref. 33), it is still schematic and therefore does not reproduce all features with quantitative accuracy.

detailed balance condition, $w_{i,f}$ should facilitate a realistic description of thermally activated jumps. Here we use the so-called transition dynamics algorithm (TDA) in which a single-particle jump proceeds by two successive steps via an intermediate state I with energy $E_I=\Delta+(E_i+E_f)/2$ such that $w_{i,f}=w_{i,I}w_{I,f}$. The rates have a Metropolis form $w_{j,j'}=\min[1,\exp[-(E_{j'}-E_j)/k_BT]]$ and the quantity $\Delta>0$ characterizes the effect of the (bare) saddle point of the adiabatic substrate potential. The use of the TDA is supported by recent molecular dynamics (MD) studies,[41] where it was found that the TDA is qualitatively consistent with the dynamics seen in a true microscopic model of a system consisting of interacting particles. Further details and additional references can be found in Ref. 33.

In the present study we will concentrate on the coverage dependence of the diffusion coefficients D_T and D_C at two different temperature regions below T_c, where $T_c\approx710$ K is the critical temperature between the high temperature disordered phase and the low temperature $p(2\times1)$ ordered phase around $\theta=0.5$.[38] These regions are characterized by the following features (see Fig. 1).

(1) The first temperature region around 590 K is characterized by a disordered phase (DO) at low coverages, from which it crosses over to an ordered $p(2\times1)$ phase at $\theta=0.35$. At higher coverages, there is another transition to an ordered $p(2\times2)$ phase at $\theta=0.59$, which in turn crosses over to a disordered phase at $\theta=0.78$. All these transitions are continuous.

(2) In the second region around 465 K, there is again a disordered phase at very low coverages. At $0.12\leqslant\theta\leqslant0.45$, however, there is a coexistence phase of the DO and the $p(2\times1)$ phases as bounded by first order phase transition boundaries. The $p(2\times1)$ phase around $\theta=0.5$ then crosses continuously over to the $p(2\times2)$ phase at $\theta=0.63$, which in

turn crosses continuously over to the disordered phase at $\theta = 0.81$.

In both cases, we calculate all quantities of interest at three different temperatures centered around 590 K and 465 K, which allows a determination of the effective diffusion barriers. The system size used is typically 30×30, although larger system sizes have also been used to study finite size effects around phase transition boundaries.

III. RESULTS FOR TRACER DIFFUSION

We first consider the motion of a single tagged particle in the presence of other particles as a function of the coverage θ. For fixed coverage in the hydrodynamic regime, it is characterized by the tracer diffusion coefficient[3]

$$D_T = \lim_{t\to\infty} \frac{1}{4Nt} \sum_{i=1}^{N} \langle |\vec{r}_i(t) - \vec{r}_i(0)|^2 \rangle, \tag{1}$$

which accounts for all the diffusing particles $i=1,\ldots,N$, and is defined in terms of their positions $\vec{r}_i(t)$ at time t. Note that D_T is actually a tensor quantity; for the purposes of the present work we use a simple scalar notation. Then, within the lattice-gas description, a formally exact way of describing the temperature and coverage dependent tracer diffusion coefficient $D_T(\theta,T)$ is to write it as[13,15]

$$D_T(\theta,T) = \frac{a^2}{4}\Gamma(\theta,T) f_T(\theta,T), \tag{2}$$

where a is the jump length of individual (nearest neighbor) jumps and $\Gamma(\theta,T)$ is the average transition rate of such single-particle jumps. The term $f_T(\theta,T)$ is a correlation factor containing *all* memory effects (correlations not included in Γ already). The approximation where $f_T \equiv 1$ is called the dynamical mean field (DMF) theory for D_T.[15,16] The decomposition in Eq. (2) allows a convenient estimation of the actual memory effects.

A. Overall behavior of D_T

The tracer diffusion coefficient D_T and the jump rate Γ were numerically computed throughout the coverage range at $T=590$ K, while in the lower temperature region around 460 K only Γ was studied in detail. The high temperature results are shown in Fig. 2(a). First, we note that D_T and the DMF approximation $a^2\Gamma/4$ are in good qualitative agreement. This implies that the overall behavior of D_T arises mainly from the kinetic factor Γ. Similar results have been found in previous studies of some adsorption systems[13,15,16,20] as well as for more complex models of chainlike molecules.[15,16]

B. Coverage dependence of f_T

The difference between D_T and $a^2\Gamma/4$ in Fig. 2(a) shows that memory effects are considerable in the ordered phases, and thus a precise evaluation of $f_T(\theta,T)$ is necessary. This function is very difficult to calculate analytically for an interacting system, and thus numerical simulations have usually been employed.[20,42–45] However, in the special case of the Langmuir gas model,[12] in which the only interaction between diffusing particles is the exclusion of double occupancy of lattice sites, the corresponding correlation factor $f_T^L(\theta)$ can be analytically estimated in various lattice geometries.[46–52] For the Langmuir gas, $\Gamma(\theta)=\nu(1-\theta)$, where ν is the bare single-particle jump rate and $(1-\theta)$ represents the blocking effect of occupied sites. The decomposition corresponding to Eq. (2) can now be written in the form

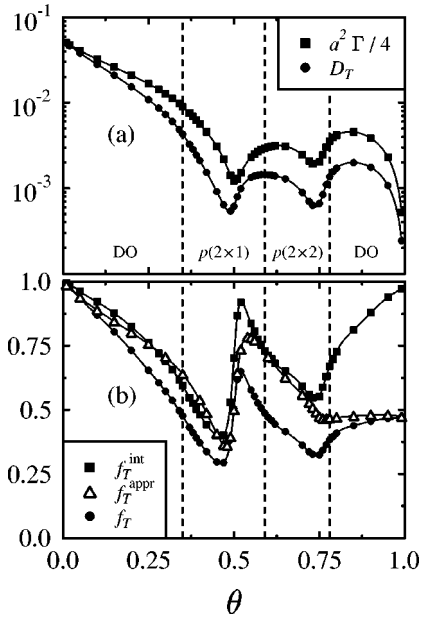

FIG. 2. (a) Results for $D_T(\theta,T)$ (circles) and $a^2\Gamma(\theta,T)/4$ (squares) at $T=590$ K. (b) Results for the tracer correlation factors at $T=590$ K. Shown are $f_T(\theta,T)$ (circles) as determined directly from the MC simulations, the correlation factor $f_T^{\rm int}(\theta,T)$ arising from direct interparticle interactions (squares), and the approximate correlation factor $f_T^{\rm appr}(\theta,T)$ (triangles) based on Eq. (6). The critical coverages of second order phase transition boundaries are shown with dashed lines. Error bars here and in the following figures are smaller than the size of the symbols, if not separately shown.

$$D_T(\theta) = \frac{a^2}{4}\nu(1-\theta) f_T^L(\theta) \equiv D_T^{\rm MF}(\theta) f_T^L(\theta), \tag{3}$$

where $D_T^{\rm MF}(\theta) \equiv a^2\nu(1-\theta)/4$ is the mean-field tracer diffusion coefficient.

In the limit of $T\to\infty$ with double occupation (and desorption) excluded, any interacting lattice-gas system becomes equivalent to the Langmuir gas model with $\nu(1-\theta) = \Gamma(\theta)$, which means that $f_T(\theta,T\to\infty) = f_T^L(\theta)$ in a given geometry. This motivates the decomposition of $f_T(\theta,T)$ into the product of two contributions as $f_T(\theta,T) \equiv f_T^L(\theta) f_T^{\rm int}(\theta,T)$, the latter factor $f_T^{\rm int}(\theta,T)$ arising from *direct* interparticle interactions. To study memory effects due to the direct interactions, we then compute $f_T(\theta,T)$ numerically and separate the monotonously decaying Langmuir part $f_T^L(\theta)$ [with $f_T^L(0)=1$ and $f_T^L(1)\approx0.47$] that has been accurately computed in previous works.[13,46,48–50,52] Results at $T=590$ K shown in Fig. 2(b) reveal that indeed most of the coverage dependence of $f_T(\theta,T)$ comes from the memory effects arising from the interparticle interactions. Further, in

agreement with related simulation work,[20,42–45] we find $f_T(\theta,T)$ to have a minimum around the ideal coverages of the ordered phases.

C. Directional correlations in single-particle jumps

Overall, the memory effect displayed in Fig. 2 has a tendency to decrease the value of D_T. This suggests that the memory effect in the present system is somehow related to the well-known back-correlation mechanism, in which the diffusing particle after its previous jump has a larger probability to jump backwards than to the other directions. To see whether this is really the case, we consider the correlations between consecutive single-particle jumps in detail.

A convenient way to study the correlations between successive jumps is to consider *directional correlations* between two jumps separated by m previous jumps by a tagged particle. To this end, we compute the probability that the $(n+m)$th jump is made to the same $[p_\uparrow(m)]$ or to the opposite direction $[p_\downarrow(m)]$, or to the left $[p_\leftarrow(m)]$ or to the right $[p_\rightarrow(m)]$ with respect to the nth jump. In the absence of any directional correlations, all these four probabilities would be equal. Even in the Langmuir gas, however, the exclusion rule gives rise to nontrivial back-correlation effects as is evident from Fig. 3(a). In our interacting system within the ordered phases, the directional correlations are further enhanced as demonstrated by the results in Figs. 3(b) and 3(c). They are clearly dominated by $p_\downarrow(m)$ and $p_\uparrow(m)$, while the role of $p_\leftarrow(m)$ and $p_\rightarrow(m)$ is very weak. This is mainly due to the structure of the ordered phases as demonstrated by the configuration snapshots in Fig. 1, and also due to the tendency of the system to form one-dimensional vacancy clusters in the $p(2\times2)$ phase.

To further quantify the directional correlations between two jumps separated by m previous jumps by a tagged particle, we define

$$P(\theta,T,m)\equiv p_\downarrow(\theta,T,m)-p_\uparrow(\theta,T,m),\quad m\geqslant 1. \tag{4}$$

This quantity is closely connected to earlier analytical works for the Langmuir gas model,[46–51] where in the high coverage limit $\theta\rightarrow 1$,

$$f_T^L=\frac{1+\langle\cos\phi\rangle}{1-\langle\cos\phi\rangle} \tag{5}$$

is the correlation factor for *vacancy diffusion*, and ϕ is the angle between two consecutive single-particle jumps. In this case, $\langle\cos\phi\rangle=-P(\theta\rightarrow 1,1)$. If we assume that the predominant memory contribution for tracer diffusion comes from the back-correlation between two consecutive $(m=1)$ single-particle jumps, we can generalize Eq. (5) as

$$f_T^{\mathrm{appr}}(\theta,T)=\frac{1-P(\theta,T,1)}{1+P(\theta,T,1)}, \tag{6}$$

where $P(\theta,T,1)$ is now calculated numerically from the model system in question for all coverages. Results using this approximation are shown in Fig. 2(b) and they indicate that $f_T^{\mathrm{appr}}(\theta,T)$ yields a surprisingly good estimate of the true correlation factor $f_T(\theta,T)$.

While the results in Fig. 2(b) and Fig. 3 clearly demonstrate the importance of the back-correlation mechanism,

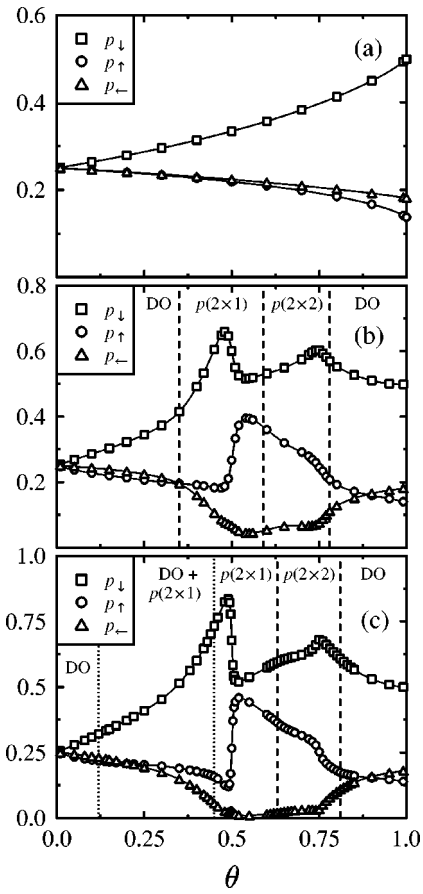

FIG. 3. (a) Normalized probabilities (with $m=1$) for a jump backward ($p_\downarrow$), forward ($p_\uparrow$), to the left ($p_\leftarrow$), and to the right ($p_\rightarrow$) with respect to the reference jump in (a) the Langmuir gas model, at (b) $T=590$ K, and at (c) $T=460$ K. The probabilities $p_\leftarrow$ and $p_\rightarrow$ are equal due to symmetry. The critical coverages of first and second order phase transition boundaries are shown with dotted and dashed lines, respectively.

considering correlations up to $m=1$ only is not adequate for a quantitative description of the directional correlation effects. The behavior of $P(\theta,T,m)$ for different values of m shown in Fig. 4(a) and Fig. 4(b) illustrates this fact very clearly. We first observe that the range of memory effects is rather long, and will be analyzed in detail in Sec. III D. We also find that the directional correlations are most pronounced in the ordered phases, and in particular in the $p(2\times1)$ phase right below the ideal coverage $\theta=0.5$. There, as illustrated by the configuration snapshots in Fig. 5, the adatoms are wandering in the $p(2\times1)$ structure which is locally broken by a few vacant sites. These imperfections are the main reason for the very pronounced memory effect, since most of the successful jumps that facilitate long-range mass transport take place near the vacancies. After a jump the particle has a strong tendency to return to its previous site, or to wander in an effectively one-dimensional (1D) channel before filling another vacancy site. The situation is very different right *above* the ideal coverage. At these coverages, the $p(2\times1)$ structure is almost perfect, and the few additional adatoms perform almost 1D random walk motion along the channels. These considerations explain the behavior of $f_T(\theta,T)$ around $\theta=0.5$ as shown in Fig. 2(b), with a minimum just below and a maximum just above $\theta=0.5$.

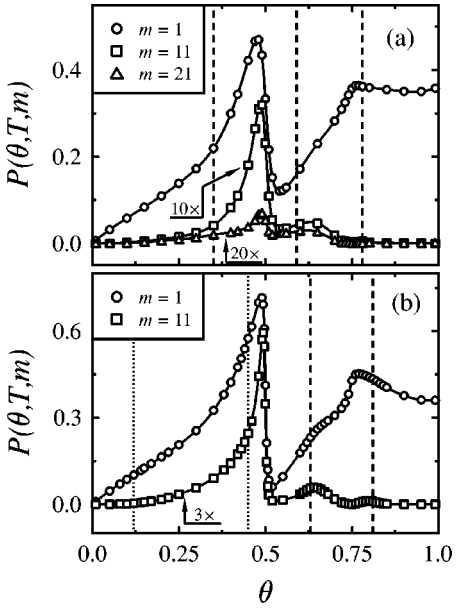

FIG. 4. Results for $P(\theta,T,m)$ as a function of coverage with various values of m at (a) $T=590$ K and (b) $T=460$ K. Note that the scale for some of the curves has been expanded to clarify the presentation. The critical coverages of first and second order phase transition boundaries are shown with dotted and dashed lines, respectively.

Other parts of the phase diagram, where the memory effects turn out to be nontrivial, are the boundaries of *second order* phase transitions. Here the memory effects are not as strong as deep inside the ordered phases. As an example, we consider Fig. 4(b), where $P(\theta,T,m)$ is shown at $T=460$ K for two values of m. In particular, $P(\theta,T,11)$ shows weak maxima at phase transition boundaries around $\theta=0.64$ and $\theta=0.80$. Close to the boundaries of first order phase transitions ($\theta=0.12$ and $\theta=0.45$), however, no such effects are observed.

D. Decay of the directional correlations

To consider the temporal decay of the memory effects and directional correlations, we first define

$$\Sigma_P(\theta,T,k)\equiv\sum_{i=1}^{k} P(\theta,T,2i-1), \tag{7}$$

which is simply the cumulative sum of $P(\theta,T,m)$ for all odd m.[53] For large k, $\Sigma_P(\theta,T,k)$ converges to some limiting value, since $P(\theta,T,m)$ should decay to zero asymptotically. The time after which the directional correlations die out is related to the decay of the memory function and in the present case it should be of the same order as the onset of the hydrodynamic regime τ_H, after which the mean-square displacement in Eq. (1) is linear in time as required in the determination of the true hydrodynamic diffusion coefficient D_T via Eq. (1).[36] Knowledge of the quantity τ_H and its dependence on the interactions and coverage has therefore a lot of relevance in both simulations and experiments.

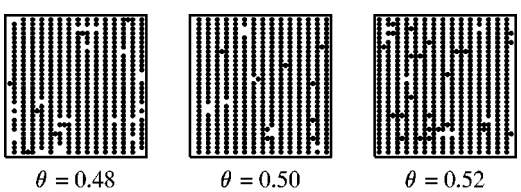

FIG. 5. Representative snapshots of the configurations in the $p(2\times1)$ phase in the O/W(110) system at $T=590$ K and around the coverage 0.50. The occupied sites are denoted by filled circles.

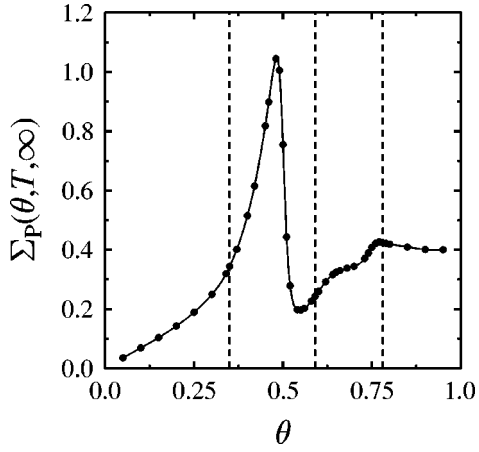

FIG. 6. Results for $\Sigma_P(\theta,T,\infty)$ [defined in Eq. (7)] as a function of coverage at $T=590$ K. Note the similar features between $\Sigma_P(\theta,T,\infty)$ shown here and $f_T(\theta,T)$ in Fig. 2(b). The critical coverages of second order phase transition boundaries are shown with dashed lines.

The qualitative behavior of $\Sigma_P(\theta,T,\infty)$ shown in Fig. 6 can be understood on the basis of the memory effects discussed in the preceding section. The large peak just below $\theta=0.5$ is due to the high degree of back-correlations, while the sharp dip above $\theta=0.5$ indicates much weaker correlations.

To determine the quantity τ_H, we determine the point k_H, where the cumulative sum $\Sigma_P(k)$ attains 99% of its limiting value via $\Sigma_P(k_H)=0.99\Sigma_P(\infty)$.[54] We take $\tau_H=k_H/\Gamma$ then to be our operational definition for the onset of the hydrodynamical regime given in units of Monte Carlo time steps. The main advantage of using the sum $\Sigma_P(k)$ instead of $P(m)$ is the reduced noise and thus a more precise determination of the onset. The results for τ_H are given in Fig. 7. The strong influence of a second order phase transition boundary around $\theta=0.37$ is another indication of the importance of critical effects. As far as ordering is concerned, its effect is most pronounced in the $p(2\times1)$ phase where a very prominent peak appears close to the ideal coverage of one-half. In the $p(2\times2)$ phase, the value of the onset as well as the memory effects in general (see Fig. 6) are not as large, thus implying that the actual microscopic structure of the adsorbate layer is also important in the characterization of memory effects. Nevertheless, it turns out that the behavior of τ_H is dominated by the number of successful jumps via k_H, since $1/\Gamma$ also shown in Fig. 7 cannot explain all features in τ_H. Thus, the quantity Γ alone, which is easy to determine from both simulations and experiments, is unfortunately not enough to predict the behavior of τ_H.

Next, we show results for the actual decay of the directional correlations as a function of the number of jumps m. Figure 8 shows the decay of $P(m)$ at two coverages at $T=590$ K. After a crossover period whose width increases

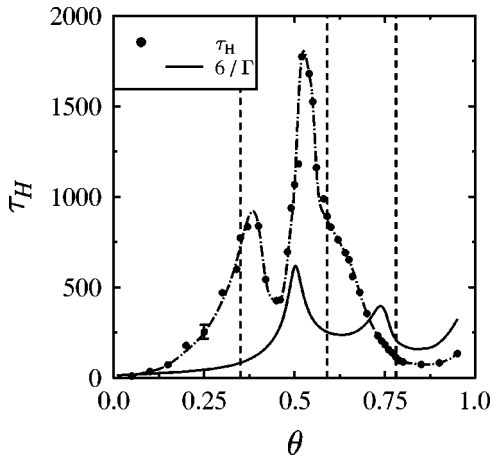

FIG. 7. Results for the onset of the hydrodynamical regime τ_H as a function of coverage at $T=590$ K. The time is given in units of Monte Carlo time steps $\tau_H=k_H/\Gamma$ (see text). The behavior of the inverse transition rate $1/\Gamma$ is also shown for comparison purposes. The critical coverages of second order phase transition boundaries are shown with dashed lines.

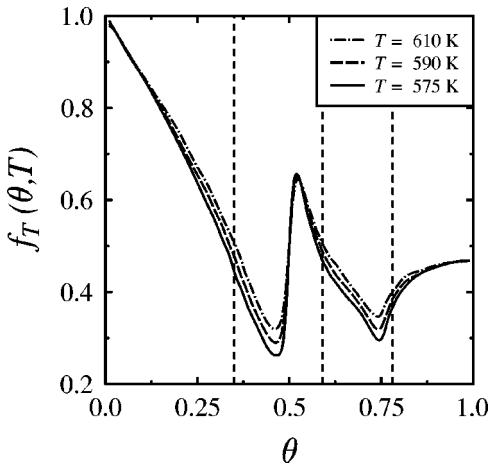

FIG. 9. Results for $f_T(\theta,T)$ at three different temperatures below T_c to illustrate the temperature dependence of the memory factor. The critical coverages of second order phase transition boundaries are shown with dashed lines.

with larger values of k_H, we find $P(m)$ to follow a power law $P(m)\sim m^{-x}$ with an exponent $x\approx 1.5$. This decay at intermediate times holds up to $m<k_H$, followed by another, rather wide crossover region around k_H. At times beyond τ_H, the decay changes to some other characteristic form. Our best results are consistent with the assumption that the asymptotic long-time behavior of $P(m)$ is governed by an exponential $P(m)\sim\exp(-m/\tau_m)$ as shown in the inset of Fig. 8(b). However, the nature of the asymptotic decay is very difficult to determine accurately.

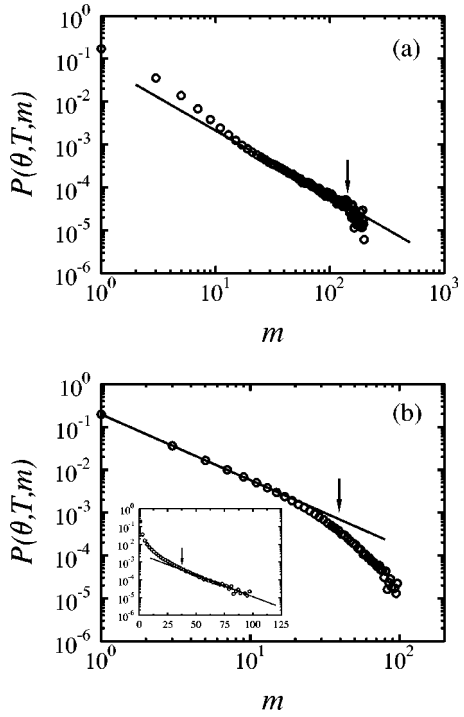

FIG. 8. Representative results for the decay of $P(\theta,T,m)$ at (a) $\theta=0.30$ and (b) $\theta=0.62$ vs the number of successful jumps m at $T=590$ K. Here results with only odd values of m are shown. The arrows indicate the onset k_H as determined from a 99.9% criterion $[\Sigma_P(k_H)=0.999\Sigma_P(\infty)]$. The linear full curves are power-law fits to the data with an exponent $x=-1.53\pm0.01$ in both cases. In the inset of (b), we furthermore show the exponential decay and the corresponding fit of $P(\theta,T,m)$ at large times.

These observations are consistent with our recent more general study[36] of dynamical correlations, in which we introduced a ''memory expansion'' of the relevant displacement correlation functions through which diffusion coefficients can be computed. This ''memory expansion'' approach can be applied to lattice-gas models as well as continuous models. In Ref. 36, several different strongly interacting systems were considered and, in all cases, a power-law decay of correlations between center-of-mass displacements as well as single-particle displacements in the intermediate time regime was found. The exponent x characterizing this power-law decay for all the systems studied so far has a value of about 1.5 and was only weakly dependent on the coverage. The agreement of these results with the present result found for the directional correlation decay is nontrivial, since the two approaches are very different. Further studies about the possible universal nature of memory effects are in progress.[55]

E. Memory effects in the effective diffusion barriers

A convenient way to analyze the temperature dependence of the diffusion coefficient is to fit it to the activated Arrhenius form. In this context, it is often assumed that the effective activation barrier E_A^T for tracer diffusion arises entirely from the thermally activated nature of a single-particle jump rate Γ. However, a strong temperature dependence of the correlation factor $f_T(\theta,T)$ can result in an additional contribution to E_A^T. This is indeed the case in our model system as shown in Fig. 9, where $f_T(\theta,T)$ varies rapidly as a function of T (note the small temperature difference between adjacent curves), especially near the optimal coverages 0.5 and 0.75 of the $p(2\times1)$ and $p(2\times2)$ phases.

To characterize the importance of memory effects in the observed activation barriers, we follow the common practice in defining the effective tracer diffusion barrier E_A^T as the local slope of D_T in an Arrhenius plot:

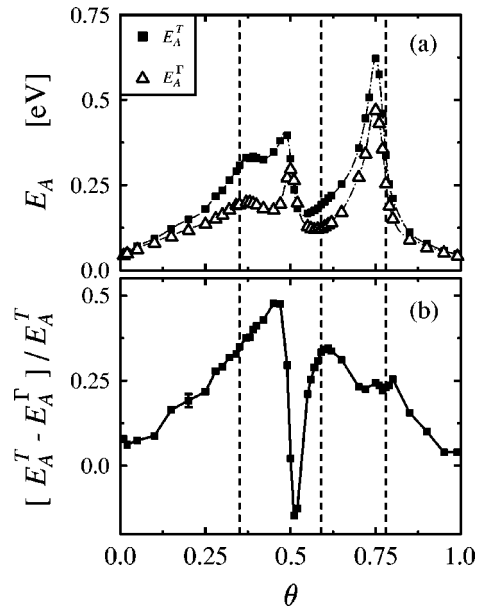

FIG. 10. (a) Results for the barriers E_A^T and E_A^Γ as determined around 590 K. (b) The relative contribution of memory effects (via the quantity $[E_A^T - E_A^\Gamma]/E_A^T$) in the tracer diffusion barrier E_A^T. The critical coverages of second order phase transition boundaries are shown with dashed lines.

$$E_A^T(\theta,T) \equiv -\frac{\partial}{\partial(1/k_B T)} \ln D_T(\theta,T). \tag{8}$$

Similarly we define a jump rate barrier $E_A^\Gamma(\theta,T)$ as the local slope of $\ln \Gamma(\theta,T)$ vs $1/k_B T$. The effective barriers E_A^T and E_A^Γ are shown in Fig. 10(a), where the influence of critical effects and ordering is again evident. However, despite the qualitative similarity between E_A^T and E_A^Γ, their quantitative agreement is not good. This difference is entirely due to the memory effects [see Eq. (2)].

As shown in Fig. 10(b), the role of memory effects in E_A^T is most important near phase transition boundaries and within the ordered phases. In these regimes, we find perhaps surprisingly that up to about 25–50 % of the effective barrier E_A^T comes from the memory contribution, which arises from temperature variations in f_T (see Fig. 9). Even at low coverages $\theta < 0.20$, the memory contribution to the effective barrier E_A^T is about 5–20 %, and increases at lower temperatures where the role of interparticle interactions becomes more important.[56]

The explicit relation of the effective barriers E_A^Γ and E_A^T to the microscopic activation barriers remains unclear. However, our results allow us to make certain qualitative interpretations concerning the origin of the effective barriers. First, the distribution of microscopic barriers is typically very complex,[33] thus E_A^Γ at a finite coverage somehow results from a complex average of all instantaneous activation barriers. Furthermore, we find that in the limit $\theta \to 0$, E_A^Γ is approximately equal[34] to the barrier[33] E_A^W extracted from a single-particle waiting-time distribution,[57] which in turn is related to the most expensive activation process in tracer diffusion.[33] The barriers E_A^Γ and E_A^W are approximately similar also at finite coverages,[34] thus studies of E_A^Γ can provide information of the limiting activation processes in single-particle motion. This is particularly useful in experimental studies of surface diffusion at finite coverages, where (unlike the waiting-time distribution) the transition rates are relatively easy to measure. What makes the interpretation more difficult, however, is the fact that in the vicinity of phase transition boundaries entropic effects lead to rapid temperature variations in Γ,[33] yielding therefore an additional contribution to E_A^Γ. In the present work, this effect is slightly pronounced at $\theta \approx 0.35$ and very prominent in the region $0.67 \leqslant \theta \leqslant 0.81$.[58] Thus in these regions E_A^Γ is not *directly* connected to any dominating microscopic activation process. Evidently the behavior of E_A^T, in which the memory contribution is also included, is even more complicated.

IV. RESULTS FOR COLLECTIVE DIFFUSION

We next consider the collective diffusion coefficient D_C as given by the Kubo-Green relation[3]

$$D_C = \xi \lim_{t\to\infty} \frac{1}{4Nt} \left\langle \left| \sum_{i=1}^{N} [\vec{r}_i(t) - \vec{r}_i(0)] \right|^2 \right\rangle \equiv \xi D_{\text{c.m.}}, \tag{9}$$

where $D_{\text{c.m.}}$ is the dynamic term arising from the center-of-mass (c.m.) motion, and the ''thermodynamic factor'' $\xi = \langle N \rangle / \langle (\delta N)^2 \rangle$ descibes the particle number fluctuations in the overlayer.[3] Again, within the lattice-gas description, one can write a formally exact decomposition of D_C into different contributions as[13,15]

$$D_C(\theta,T) = \frac{a^2}{4} \xi(\theta,T) \Gamma(\theta,T) f_C(\theta,T). \tag{10}$$

In analogy to the case of tracer diffusion, setting the c.m. correlation factor $f_C \equiv 1$ corresponds to the DMF theory, with no memory effects included.[15,16] This is the case in the Langmuir gas model with nearest neighbor jumps where D_C is constant for $0 \leqslant \theta \leqslant 1$.[59,60] In the presence of direct interparticle interactions, DMF has been shown to give a very good approximation of the true D_C since memory effects arising from the c.m. motion are typically much weaker than those for tracer particles.[15,16]

A. Overall behavior of D_C

Results for $D_{\text{c.m.}}$ and ξ together with the resulting collective diffusion coefficient D_C are shown in Figs. 11(a) and 11(b) for $T = 590$ K and 465 K, respectively. The c.m. and the thermodynamic contributions are clearly competing, and it turns out that at low temperatures, the thermodynamic factor ξ dictates the qualitative behavior of the coverage dependence of D_C. Similar results for other lattice-gas systems have been found by Danani *et al.*[26] The most illustrative example of this behavior is shown in Fig. 11(b), where near the first order phase transition boundaries ξ has a very dramatic change at the critical coverages. Near a second order phase boundary, $(\partial\mu/\partial\theta)_T \to 0$ and thus the thermodynamic factor ξ is expected to diverge at the critical field μ_c.[61] Actually what we see in Fig. 11(b) is only a weak maximum in ξ and D_C at the second order phase boundary. This is due to the relatively small system size $L = 30$ that suppresses long-wavelength fluctuations in this case.[62]

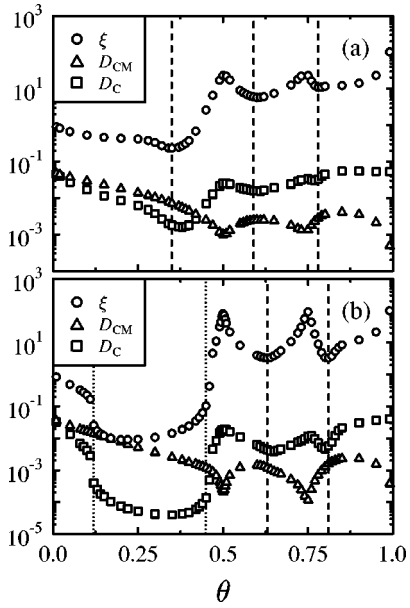

FIG. 11. Results for $D_{\text{c.m.}}$, ξ, and D_C at (a) $T=590$ K and (b) $T=465$ K. The critical coverages of first and second order phase transition boundaries are shown with dotted and dashed lines, respectively.

We wish to emphasize that the present case should not be regarded as a generic one. Between the two competing factors, $D_{\text{c.m.}}$ and ξ, the dominant one that dictates the coverage dependence of D_C depends on the coverage and the temperature as well as the particular nature of the system. In the temperature regimes of the present study, we find the coverage dependence of ξ to be stronger than that of $D_{\text{c.m.}}$, while for some other systems the situation can be the opposite. This conclusion is supported by experimental results, where both local minima and maxima of D_C have been observed around coverages of fully ordered phases.[3,5,28,29,63,64] These two cases correspond to a situation where either $D_{\text{c.m.}}$ or ξ wins, respectively.

B. Coverage dependence of f_C

We next consider the importance of memory effects in the c.m. motion. Using results for $D_{\text{c.m.}}(\theta,T)$ and $\Gamma(\theta,T)$, we obtain the collective memory factor $f_C(\theta,T)$ shown in Fig. 12. In the Langmuir gas model, the corresponding memory factor $f_C^L(\theta)\equiv 1$ for $0\leqslant\theta\leqslant 1$.[59] It turns out that the behavior of f_C across the phase diagram is qualitatively similar to that of f_T in Fig. 2(b). They both have minima at coverages corresponding to the fully ordered phases, although this feature is much weaker in f_C. It is also evident that the memory effects in the c.m. motion are not of great significance around phase transition boundaries. In the coexistence phase at $0.12\leqslant\theta\leqslant 0.45$ in Fig. 12(b), the memory effects tend to slightly increase with an increasing coverage. The same holds true around second order phase transition boundaries.

We want to emphasize that the dynamics behind $D_{\text{c.m.}}$ and D_T are very different. In collective diffusion, the motion of the c.m. results from the jumps of *different* particles at different times. Thus it is clear that the consecutive displacements of the c.m. are less correlated than the corresponding displacements of a tagged particle considered in tracer diffusion, an idea that is in agreement with the results shown in Figs. 2(b) and 12(a). While the quantity f_C may be very difficult to compute analytically, this observation is very useful since the c.m. term $D_{\text{c.m.}}$ is thus very well approximated by the jump rate Γ. This can be utilized in computational and experimental work on collective diffusion (for further discussion see Refs. 15,16).

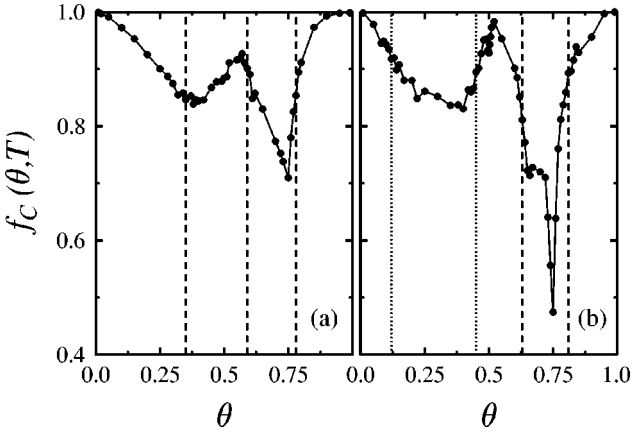

FIG. 12. Results for $f_C(\theta,T)$ at (a) $T=590$ K and (b) $T=465$ K. The error bars are about the size of the symbols. The critical coverages of first and second order phase transition boundaries are shown with dotted and dashed lines, respectively.

C. Memory effects in the barrier E_A^C

The activation barriers for collective diffusion as extracted from the Arrhenius analysis of D_C are shown in Figs. 13(a) and 13(c). In agreement with the discussion above, we find the effective barrier $E_A^{\text{c.m.}}$ of $D_{\text{c.m.}}$ not to be able to completely explain the coverage dependence of the effective activation barrier E_A^C for collective diffusion. Instead, the behavior of E_A^C in the present case comes mainly from the nonactivated, rapid temperature variations in ξ. The subtle point concerning the competition between $D_{\text{c.m.}}$ and ξ is illustrated even in the framework of the present model system, in which ξ does not dominate the behavior of E_A^C in all situations. Namely, when one crosses the phase transition boundary between the $p(2\times 1)$ phase and the disordered region around 710 K near $\theta\approx 0.5$, the barrier E_A^C arises mainly from temperature variations in $D_{\text{c.m.}}$[33]

To quantify the memory contribution in E_A^C, we use the difference between $E_A^{\text{c.m.}}$ and E_A^Γ. As shown in Fig. 13(b), the memory contribution in the c.m. barrier $E_A^{\text{c.m.}}$ is typically about 10% and thus less important but also more complicated than in E_A^T. A more detailed microscopic analysis of the variation of the memory contribution in $E_A^{\text{c.m.}}$ is unfortunately very difficult due to the weakness of the memory effects. However, the weak role of memory effects in collective diffusion can again be of great use to understanding of experimental data. Namely, it implies that $E_A^{\text{c.m.}}\approx E_A^\Gamma$ is valid to a good approximation, and therefore one can extract information of the most expensive single-particle diffusion processes by studying the temperature dependence of $D_{\text{c.m.}}$ This is possible, e.g., in Gomer's fluctuation method.[3]

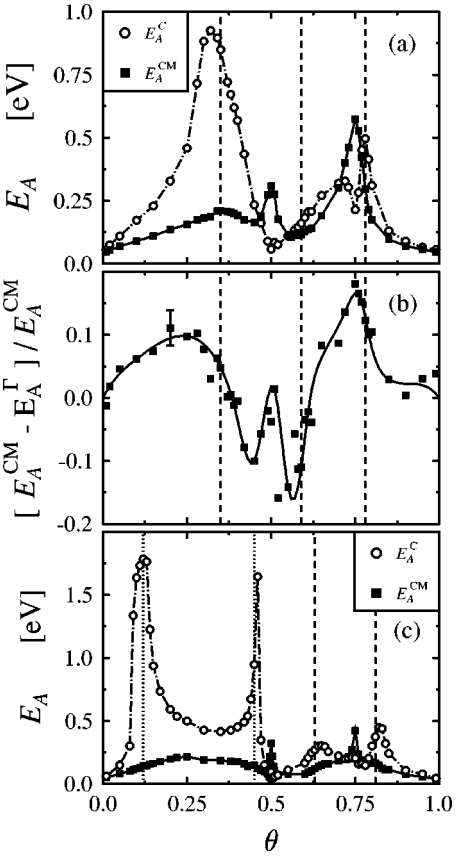

FIG. 13. (a) Results for the Arrhenius barriers E_A^C for D_C and $E_A^{\text{c.m.}}$ for $D_{\text{c.m.}}$ as determined around 590 K. (b) The relative contribution of memory effects (via the quantity $[E_A^{\text{c.m.}}-E_A^\Gamma]/E_A^{\text{c.m.}}$) in the c.m. barrier $E_A^{\text{c.m.}}$ around 590 K [cf. (a)], where the full line is only to guide the eye. (c) Corresponding barriers as determined around 465 K. The critical coverages of first and second order phase transition boundaries are shown with dotted and dashed lines, respectively.

D. Comparison of E_A^C with experimental data

The O/W(110) system is one of the best known adsorption systems.[3,39] In addition to a vast amount of numerical simulation data, there are also various experimental studies of the diffusion coefficient in this system. Concerning the activation barriers, the most systematic study is by Nahm and Gomer,[37] who have determined the Arrhenius parameters for collective diffusion around 500–600 K. The number of data points does not allow a thorough comparison with our work, but let us summarize their main results. The c.m. barrier $E_A^{\text{c.m.}}$ was found to increase at low coverages towards a maximum of 0.9 eV that appeared around $\theta=0.40$. At higher coverages, there were just two data points at coverages of 0.56 and 0.72 that were approximately of equal magnitude. These results are consistent with our simulation data in Fig. 13(a). Thus we conclude that the present model is able to grasp the main features of the dynamic contribution $E_A^{\text{c.m.}}$ As we emphasized before, the ingredients of the theoretical model here consist not just of the lattice-gas Hamiltonian but also of the choice of the transition rate between different configurations. The importance of a proper description of dynamics becomes particularly clear when our results are compared with another Monte Carlo (MC) study,[27] whose results for the activation barriers were different. In the model used there,[27] the phase diagram consists only of the $p(2\times1)$ and the disordered phases, and the dynamics was introduced by using the initial value approach. By comparing MD results with various schemes that are commonly used to introduce the dynamics into the lattice-gas model MC simulations, we found that the present TDA approach gives results that are consistent with MD results, while the initial value dynamics yields results that are qualitatively incorrect in many cases.[41]

The comparison between theory and experiment of the collective diffusion barrier E_A^C, which includes the thermodynamic contribution, is a different matter. Experimental data for E_A^C are approximately identical with $E_A^{\text{c.m.}}$, thus implying a negligible temperature dependence of ξ. Simulation results presented here as well as previous studies yield very different results. To explain the discrepancy, Nahm and Gomer suggested[37] that polaronic effects, which are not included in the lattice-gas descriptions, could play a role in determining ξ. Another explanation is the relatively small probe size of about 350 nm^2 used in the field emission fluctuation experiment that could prevent the observation of the long-wavelength particle number fluctuations which contribute significantly to ξ.

V. SUMMARY AND DISCUSSION

To summarize, we have studied various aspects of memory effects in a strongly interacting lattice-gas model system appropriate for the description of the O/W(110) system. We have first determined the coverage dependence of correlation factors for tracer and collective diffusion and analyzed their dependence on ordering and critical effects. Furthermore, we have developed a microscopic picture of memory effects as they appear in tracer diffusion. Our results based on directional correlations between single-particle jumps clearly show that the back-jump correlation mechanism gives the leading contribution to the memory effects in tracer diffusion. They also illustrate the important role ordering and critical effects play at short-time scales where the memory effects are most pronounced. In this regard, the full memory effects as described by the correlation factors are affected mostly by the ordering of the adlayer, while the importance of critical effects is best illustrated in the decay of directional correlations. The decay is characterized by a power law at times prior to the onset of the hydrodynamic regime, while at times beyond the onset, it is exponential.

Besides studying the coverage dependence of memory effects, we also determined their dependence on temperature in low temperature ordered phases. This aspect addresses an important question of how large the memory contribution is in the effective barriers extracted from an Arrhenius analysis of experimental data. Within the lattice-gas model, we find that the tracer diffusion barrier E_A^T contains a prominent memory contribution arising from temperature variations in the correlation factor. This contribution to E_A^T is most pronounced within ordered phases and near phase transition boundaries, where interparticle interactions are the strongest. The contribution to the effective diffusion barrier from memory effects can be as large as the effective jump rate barrier E_A^Γ. For collective diffusion, the memory contribu-

tion to the effective barrier is smaller. Nevertheless, these results imply that only in rare special cases can a barrier extracted from the Arrhenius analysis be directly related to some particular thermally activated microscopic single-particle process.

Most of the existing theoretical work on diffusion in interacting systems concentrates on the overall temperature and coverage dependence of the diffusion coefficients. In numerical simulations it is possible to evaluate the relative importance of the various physical contributions such as the average jump rate, memory effects, and thermodynamic effects. In strongly interacting cases with order present, the interplay of all these factors leads to a very complicated overall behavior as demonstrated in the present study. Among the different factors, the role of the microscopic jump rate is rather well understood theoretically within the framework of the dynamical mean-field theory.[15,16] Also, the thermodynamic contribution via particle number fluctuations is an equilibrium property and has been extensively studied. The memory effect, which is the focus of the present study, is truly dynamic in origin and the one least understood. Fortunately, the microscopic origin of the memory effects can now be studied, not only via realistic computer simulations, but also by recently developed experimental techniques such as scanning tunneling microscopy. Such experimental studies of memory effects would be most desirable.

ACKNOWLEDGMENTS

The authors thank the Helsinki Institute of Physics at the University of Helsinki for computing resources. This work has in part been supported by the Academy of Finland.

*Author to whom correspondence should be sent. Present address: Department of Chemistry, Technical University of Denmark, Building 207, DK-2800 Lyngby, Denmark. Electronic address: Ilpo.Vattulainen@csc.fi

[1] J. Krug, Adv. Phys. **46**, 139 (1997).
[2] D. L. Freeman and J. D. Doll, J. Chem. Phys. **78**, 6002 (1983).
[3] R. Gomer, Rep. Prog. Phys. **53**, 917 (1990).
[4] T. Ala-Nissila and S. C. Ying, Prog. Surf. Sci. **39**, 227 (1992).
[5] *Surface Diffusion: Atomistic and Collective Processes*, edited by M. C. Tringides (Plenum, New York, 1997).
[6] L. Y. Chen and S. C. Ying, Phys. Rev. Lett. **71**, 4361 (1993).
[7] L. Y. Chen and S. C. Ying, Phys. Rev. B **49**, 13 838 (1994).
[8] L. Y. Chen, M. R. Baldan, and S. C. Ying, Phys. Rev. B **54**, 8856 (1996).
[9] A. P. Graham, F. Hofmann, J. P. Toennies, L. Y. Chen, and S. C. Ying, Phys. Rev. Lett. **78**, 3900 (1997).
[10] S. Yu. Krylov, A. V. Prosyanov, and J. J. M. Beenakker, J. Chem. Phys. **107**, 6970 (1997); J. J. M. Beenakker and S. Yu. Krylov, Surf. Sci. **411**, L816 (1998).
[11] M. Azzouz, H. J. Kreuzer, and M. R. A. Shegelski, Phys. Rev. Lett. **80**, 1477 (1998).
[12] J. B. Taylor and I. Langmuir, Phys. Rev. **44**, 423 (1933).
[13] A. Danani, R. Ferrando, E. Scalas, and M. Torri, Int. J. Mod. Phys. B **11**, 2217 (1997).
[14] I. Vattulainen, J. Merikoski, T. Ala-Nissila, and S. C. Ying, Phys. Rev. Lett. **80**, 5456 (1998); C. Uebing and V. P. Zhdanov, *ibid.* **80**, 5455 (1998).
[15] T. Hjelt, I. Vattulainen, J. Merikoski, T. Ala-Nissila, and S. C. Ying, Surf. Sci. **380**, L501 (1997).
[16] T. Hjelt, I. Vattulainen, J. Merikoski, T. Ala-Nissila, and S. C. Ying, Surf. Sci. **402–404**, 253 (1998).
[17] M. Bowker and D. A. King, Surf. Sci. **71**, 583 (1978).
[18] D. A. Reed and G. Ehrlich, Surf. Sci. **102**, 588 (1981).
[19] G. E. Murch, Philos. Mag. A **43**, 871 (1981).
[20] A. Sadiq and K. Binder, Surf. Sci. **128**, 350 (1983).
[21] M. Tringides and R. Gomer, Surf. Sci. **145**, 121 (1984).
[22] C. Uebing and R. Gomer, Surf. Sci. **331-333**, 930 (1995); and references therein.
[23] Z. Chvoj, H. Conrad, and V. Cháb, Surf. Sci. **352-354**, 983 (1996).
[24] Z. Chvoj, H. Conrad, and V. Cháb, Surf. Sci. **376**, 205 (1997).
[25] P.-L. Cao, M. Qiu, and D.-H. Shi, Surf. Sci. **374**, 350 (1997).
[26] A. Danani, R. Ferrando, E. Scalas, and M. Torri, Surf. Sci. **409**, 117 (1998).
[27] C. Uebing and R. Gomer, Surf. Sci. **381**, 33 (1997).
[28] A. G. Naumovets and Yu. S. Vedula, Surf. Sci. Rep. **4**, 365 (1985).
[29] A. T. Loburets, A. G. Naumovets, N. B. Senenko, and Yu. S. Vedula, Z. Phys. Chem. (Munich) **202**, 75 (1997).
[30] E. G. Seebauer and C. E. Allen, Prog. Surf. Sci. **49**, 265 (1995).
[31] G. L. Kellogg, Surf. Sci. Rep. **21**, 1 (1994).
[32] A. Cucchetti and S. C. Ying, Phys. Rev. B **54**, 3300 (1996).
[33] I. Vattulainen, J. Merikoski, T. Ala-Nissila, and S. C. Ying, Phys. Rev. B **57**, 1896 (1998); Phys. Rev. Lett. **79**, 257 (1997).
[34] I. Vattulainen, Surf. Sci. **412-413**, L911 (1998).
[35] D. Sahu, S. C. Ying, and J. M. Kosterlitz, in *The Structure of Surfaces II*, edited by J. F. van der Veen and M. A. van Hove (Springer-Verlag, Berlin, 1988), p. 470.
[36] S. C. Ying, I. Vattulainen, J. Merikoski, T. Hjelt, and T. Ala-Nissila, Phys. Rev. B **58**, 2170 (1998).
[37] T.-U. Nahm and R. Gomer, J. Chem. Phys. **106**, 10 349 (1997); and references therein.
[38] G.-C. Wang, T.-M. Lu, and M. G. Lagally, J. Chem. Phys. **69**, 479 (1978).
[39] C. R. Brundle and J. Q. Broughton, in *The Chemical Physics of Solid Surfaces and Heterogeneous Catalysis: Chemisorption Systems*, edited by D. A. King and D. P. Woodruff (Elsevier, Amsterdam, 1990), Vol. 3A, Chap. 3.
[40] K. E. Johnson, R. J. Wilson, and S. Chiang, Phys. Rev. Lett. **71**, 1055 (1993).
[41] I. Vattulainen *et al.* (unpublished).
[42] G. E. Murch and R. J. Thorn, Philos. Mag. **35**, 493 (1977).
[43] R. Kutner, K. Binder, and K. W. Kehr, Phys. Rev. B **26**, 2967 (1982); **28**, 1846 (1983).
[44] A. Bunde and W. Dieterich, Phys. Rev. B **31**, 6012 (1985).
[45] K. W. Kehr and K. Binder, in *Applications of the Monte Carlo Method in Statistical Physics*, edited by K. Binder (Springer-Verlag, Berlin, 1987) p. 181.
[46] O. F. Sankey and P. A. Fedders, Phys. Rev. B **15**, 3586 (1977).
[47] M. Koiwa, J. Phys. Soc. Jpn. **45**, 1327 (1978).
[48] K. Nakazato and K. Kitahara, Prog. Theor. Phys. **64**, 2261 (1980).
[49] D. K. Chaturvedi, Phys. Rev. B **28**, 6868 (1983).
[50] R. A. Tahir-Kheli and R. J. Elliott, Phys. Rev. B **27**, 844 (1983).
[51] R. A. Tahir-Kheli, Phys. Rev. B **27**, 6072 (1983).

[52] R. A. Tahir-Kheli and N. El-Meshad, Phys. Rev. B **32**, 6166 (1985).

[53] Due to the back-correlation effect, $P(m)$ oscillates with small m. Thus for practical reasons, we use $P(m)$ with only odd values of m to consider the decay of directional correlations, and to define $\Sigma_P(k)$. As far as the cumulative correlation term $\Sigma_P(k)$ is concerned, we have checked that $\Sigma_P(k)$ with large k gives consistent results with the case where all terms of $P(m)$ (with both odd and even m) are summed together.

[54] We have also considered other operational definitions of k_H and found them to be consistent with the present choice.

[55] S. C. Ying *et al.* (unpublished).

[56] We have verified this by repeating some studies for D_T and Γ at $T \approx 460$ K. In this case, the memory contribution to the barrier E_A^T was found to be about 5– 25 % at coverages $\theta < 0.20$.

[57] J. W. Haus and K. W. Kehr, Phys. Rep. **150**, 263 (1987).

[58] Around $\theta = 0.75$, one finds [see Fig. 10(a)] a barrier E_A^Γ larger than the greatest instantaneous barrier (Ref. 33) of about 0.4 eV in this system. We have confirmed that this peak is due to the prominent critical effects near the $p(2\times 2)$ phase at temperatures studied here. Additional studies for E_A^W and E_A^Γ deeper within the ordered phases (around 440 K at $\theta \approx 0.75$) indicate that then $E_A^\Gamma < E_A^W$, thus confirming that the peak of E_A^Γ in Fig. 10(a) is mostly due to critical effects.

[59] R. Kutner, Phys. Lett. **81A**, 239 (1981).

[60] M. Torri and R. Ferrando, Chem. Phys. Lett. **274**, 323 (1997).

[61] J. D. Gunton, M. San Miguel, and P. S. Sahni, in *Phase Transitions and Critical Phenomena*, edited by C. Domb and J. L. Lebowitz (Academic Press, London, 1983), Vol. 8, p. 267.

[62] We found the finite size effects for ξ around second order phase transition boundaries to be rather small, while around first order phase transitions they seem to be significant. This is supported by our observations that a determination of ξ near first order phase transition boundaries becomes prohibitively difficult with larger system sizes.

[63] M. Šnábl, M. Ondřejček, V. Cháb, Z. Chvoj, W. Stenzel, H. Conrad, and A. M. Bradshaw, J. Chem. Phys. **108**, 4212 (1998).

[64] C. Cohen, Y. Girard, P. Leroux-Hugon, A. L'Hoir, J. Moulin, and D. Schmaus, Europhys. Lett. **24**, 767 (1993).